Short Papers

Matched Symmetrical Five-Port Microstrip Coupler

S. P. Yeo and F. C. Choong

***Abstract*—Other researchers have fabricated a symmetrical five-port microstrip coupler (with a double-ring structure) yielding a bandwidth of 58%. It has been found in this paper that a simple modification of the design topology allows the coupler's bandwidth to be broadened to 76%. A first-order model of the new prototype has also been developed, and tests have confirmed that close agreement can be expected between the predicted and experimental results for the coupler's scattering coefficients.**

***Index Terms*—Microstrip components.**

I. Introduction

Riblet *et al.* were the first to demonstrate the use of the symmetrical five-port coupler in "... a compact and simple six-port configuration with virtually ideal properties for precision measurements" [1, p. 153]. This component has since been adopted by other researchers for constructing six-port reflectometers that are able to yield optimum measurement performance (e.g., in [2]–[4]).

Various designs have already been proposed (e.g., in [5]–[11]) for the microstrip version of this particular coupler. According to Abouzahra [5, p. 154], "... the best and most comprehensive analysis for the symmetrical five-port circuit was published by Kim *et al.* [6]" and we shall thus utilize their paper as our reference. One of the designs explored in [6] is the single-ring-with-star structure; although de Ronde [7] claimed an octave bandwidth for such a coupler, the design Kim *et al.* managed to obtain from their optimization attempts had a predicted bandwidth of only 57%. Turning their attention to the double-ring topology instead, they later managed to fabricate in [6] a prototype with a measured bandwidth of 58%.

Riblet [8] indicated that it should, in principle, be possible to achieve further bandwidth improvements. We note that the ring-to-ring links of the double-ring structure described in [6] are aligned with the arms connecting the coupler to the external circuitry. In our previous project on a different coupler (which has sixfold rotational symmetry), we have found it helpful to introduce angular displacements for all of the ring-to-ring links [12]; the same approach will be applied here to the symmetrical five-port coupler. Fig. 1 depicts the double-ring structure under study where the microstrip lines linking the inner and outer rings are out of alignment with the external arms by 36°. Tapers are also included because the characteristic impedance of the coupler's external arms (where they meet the outer ring) may not be 50 Ω. In addition, we have developed a first-order model for predicting the entries of the coupler's scattering matrix, which, as is evident from the fivefold rotational symmetry of the composite structure and the reciprocity property of the substrate material, can be written in the following generic form:

$$\underline{S} = \begin{bmatrix} \gamma & \alpha & \beta & \beta & \alpha \\ \alpha & \gamma & \alpha & \beta & \beta \\ \beta & \alpha & \gamma & \alpha & \beta \\ \beta & \beta & \alpha & \gamma & \alpha \\ \alpha & \beta & \beta & \alpha & \gamma \end{bmatrix} \qquad (1)$$

Manuscript received July 17, 2000; revised January 16, 2001.

The authors are with the Electrical and Computer Engineering Department, National University of Singapore, Kent Ridge, Singapore 119260 (e-mail: eleyeosp@nus.edu.sg).

Publisher Item Identifier S 0018-9480(01)06132-4.

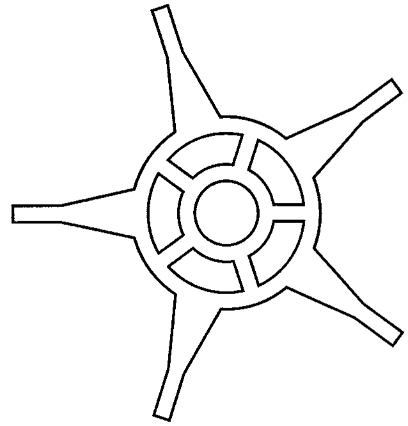

Fig. 1. Symmetrical five-port microstrip coupler with design parameters for broad-band prototype given by: inner ring—9.3-mm radius and 3.0-mm width, outer ring—16.1-mm radius and 3.5-mm width, ring-to-ring links—3.6-mm length and 5.2-mm width, tapers—13.8-mm length and 10.1- and 4.2-mm widths, substrate-relative 6.2-mm permittivity and 2.5-mm height.

where, for the ideal case [6], we require that $|\gamma| = 0$, $|\alpha| = |\beta| = 0.5$ and $\arg(\alpha/\beta) = \pm 2\pi/3$.

II. Coupler Model

We have previously employed transmission-line analysis [13] to develop a first-order eigenmode model of the symmetrical six-port microstrip coupler based on the simpler single-ring topology. The eigenmode formulation we adopted in [13] allows us to adapt the model of this rudimentary six-port structure for application to its five-port counterpart as well. The design we finally selected (after having attempted other variations of the five-port structure) is based on the more complicated topology depicted in Fig. 1 and we, therefore, need to expand on the basic model borrowed from [13] so as to account for the various additional features (*viz.* the second concentric ring, links between inner and outer rings, and tapers at external arms). We begin by listing the expressions we derived for the eigenadmittance of the coupler when operating in eigenmode of order m (where $m = 0, 1, 2$). The subscripts $\mathrm{ring1}$ and $\mathrm{ring2}$ in (2)–(4) refer, respectively, to the outer and inner rings. Table I provides the legend for the symbols used to represent the different microstrip-line and tee-junction parameters (the values of which may be calculated from the closed-form expressions collated in [14]).

A. Eigenadmittance of Coupler Without Tapers

$$(\hat{Y}_m)_C = \frac{j}{n_{\mathrm{ring1}}} \cdot \left\{ \frac{2Y_{\mathrm{ring1}}\left[\cos\left(\frac{2m\pi}{5}\right) - \cos\theta_{\mathrm{ring1}}\right] - j(\hat{Y}_m)_B \sin\theta_{\mathrm{ring1}}}{\sin\theta_{\mathrm{ring1}} + j\frac{(\hat{Y}_m)_B}{Y_{\mathrm{ring1}}}\sin^2\left(\frac{1}{2}\theta_{\mathrm{ring1}}\right)} + B_{\mathrm{ring1}} \right\} \qquad (2)$$

TABLE I
LEGEND FOR SYMBOLS EMPLOYED IN (2)–(7)

Symbol	Description of Parameter
$\hat{Y}_m$	m-th order eigen-admittance (*i.e.* admittance looking into any port of coupler operating in eigenmode of order m)
Y	characteristic admittance of microstrip line (with subscript denoting whether for inner ring, outer ring, link between rings, or taper at external arm)
θ	electrical angle of microstrip line (with subscript denoting whether for curved arc between any pair of adjacent ports or for link between rings)
$(\Delta\theta)_q$	electrical angle for short q-th element of taper
B	shunt susceptance at microstrip tee-junction (with subscript denoting location of discontinuity)
n	square of transformer ratio at microstrip tee-junction (with subscript denoting location of discontinuity)

where

$$(\hat{Y}_m)_B = n_{\rm link} Y_{\rm link} \frac{(\hat{Y}_m)_A + jY_{\rm link}\tan\theta_{\rm link}}{Y_{\rm link} + j(\hat{Y}_m)_A \tan\theta_{\rm link}} + jB_{\rm link} \quad (3)$$

$$(\hat{Y}_m)_A = \frac{j}{n_{\rm ring2}} \cdot \left\{2Y_{\rm ring2}\left[\cos\left(\frac{2m\pi}{5}\right) \operatorname{cosec}\theta_{\rm ring2} - \cot\theta_{\rm ring2}\right] + B_{\rm ring2}\right\}. \quad (4)$$

B. Eigenadmittance of Coupler with Tapers

The term $(\hat{Y}_m)_C$ in (2) represents the eigenadmittance of the coupler without the five tapers. Approximating each taper as a cascade of Q incremental steps with the qth element (where $q = 1, 2, 3, \ldots, Q$) taken as having an electrical angle of $(\Delta\theta)_q$, allows us to iteratively apply the following transmission-line formula:

$$\left(\hat{Y}_m\right)_q = Y_q \frac{\left(\hat{Y}_m\right)_{q-1} + jY_q\left(\Delta\theta\right)_q}{Y_q + j(\hat{Y}_m)_{q-1}\left(\Delta\theta\right)_q}, \qquad \text{for } q = 1, 2, 3, \ldots, Q. \quad (5)$$

$(\hat{Y}_m)_C$ is the eigenadmittance term required to initiate the iterations [i.e., for $q - 1 = 0$ in the numerator and denominator of (5)], and the final term $(\hat{Y}_m)_Q$ is the eigenadmittance of the composite coupler-with-tapers structure. We have subsequently found from our computational trials that it is important for $(\Delta\theta)_q$ to remain less than 5° for our present model.

C. Scattering Coefficients of Coupler with Tapers

Once the values of $(\hat{Y}_1)_Q$, $(\hat{Y}_2)_Q$, and $(\hat{Y}_3)_Q$ have been determined from (2)–(5), we are then able to compute the entries α, β, and γ of the coupler's 5 × 5 scattering matrix $\underline{S}$ [as defined in (1)] via the following formulas:

$$s_{ij} = \frac{1}{5}\sum_{m=0}^{m=2}(1 + \delta_{m-1} + \delta_{m-2})\lambda_m \cos\frac{2\pi m(i-j)}{5} \quad (6)$$

where δ is the Kronecker delta function and where λ_1, λ_2, and λ_3 are the corresponding eigenvalues of $\underline{S}$ given by

$$\lambda_m = \frac{1 - Z_{\rm arm}\left(\hat{Y}_m\right)_Q}{1 + Z_{\rm arm}\left(\hat{Y}_m\right)_Q}. \quad (7)$$

The characteristic admittance $Z_{\rm arm}$ of the lines connecting the composite coupler to the external circuitry has been conveniently fixed at 50 Ω for our design.

III. BROAD-BAND PROTOTYPE

The explicit formulas of (2)–(7) can be readily implemented in software form. We have since fabricated two preliminary prototypes in order to test the accuracy of the numerical results generated by our computer model. The excellent agreement between the predicted and measured results for both sets of α, β, and γ indicates that the assumptions we utilized to simplify the analysis of Section II (e.g., approximating curved arcs between adjacent ports as straight lines and ignoring the effect of parasitic coupling between neighboring discontinuities) have not given rise to any unacceptable errors over the frequency range of interest to us. To conserve space, we have not reproduced the plots for these two preliminary prototypes since neither is able to meet the $|\gamma| < 0.1$ specification adopted by Kim *et al.* [6] for defining the bandwidth of the coupler.

In view of the large number of adjustable parameters at our disposal, it is not possible for us to proceed via random trials and we have thus added an optimization subroutine, which employs the genetic algorithm expounded in [15] to minimize the following penalty function (summed over all sample frequency points f_k):

$$\xi = \sum_{k=1}^{k=K}\left\{w_\gamma\left|\gamma(f_k)\right|^2 + w_\alpha\left[\left|\alpha(f_k)\right| - \frac{1}{2}\right]^2 + w_\beta\left[\left|\beta(f_k)\right| - \frac{1}{2}\right]^2\right\}. \quad (8)$$

Fig. 2 presents the predicted and measured results for the final prototype produced by our computer-aided-design software (comprising both analysis program and optimization subroutine). The residual mismatch $|\gamma|$ of this prototype remains below 0.1 over a bandwidth of 76% (whereas for the coupler designed by Kim *et al.* "... the experimentally obtained bandwidth is about 58%" [6, p. 57]). There is, as expected from the preliminary tests' findings for our first two five-port prototypes, close correlation between the data generated by our model and the measurements taken by the HP8510C network analyzer—for magnitudes in Fig. 2(a), as well as phase differences in Fig. 2(b).

The weights selected by Kim *et al.* when implementing (8) are $w_\gamma = w_\alpha = w_\beta = 1$. We have also found that it is possible to choose other weights (e.g., $w_\gamma = 1$ and $w_\alpha = w_\beta = 0$) for the optimization runs because, as Belfort *et al.* [16] have already pointed out, α and β are related to γ for a well-designed coupler. We infer from the analysis furnished in [16] that the following bounds on the departures of α and β from their ideal-case values apply when $|\gamma|$ is sufficiently small:

$$\left||\alpha| - \frac{1}{2}\right| \le \frac{\sqrt{3}}{2}|\gamma| \quad (9)$$

$$\left||\beta| - \frac{1}{2}\right| \le \frac{\sqrt{3}}{2}|\gamma| \quad (10)$$

$$\left|\left|\arg\left(\frac{\alpha}{\beta}\right)\right| - \frac{2\pi}{3}\right| \le \frac{2}{\sqrt{3}}|\gamma|. \quad (11)$$

However, Belfort *et al.* did not provide any empirical data in [16] to establish the range of validity for their analysis. Since we have such results available, we can perform a sample check by extracting the measured data presented in Fig. 2 for $\arg(\alpha/\beta)$ at $f = 1.5, 1.6, 1.7, \ldots, 3.6$ GHz and replotting them in Fig. 3 against $|\gamma|$. It is evident

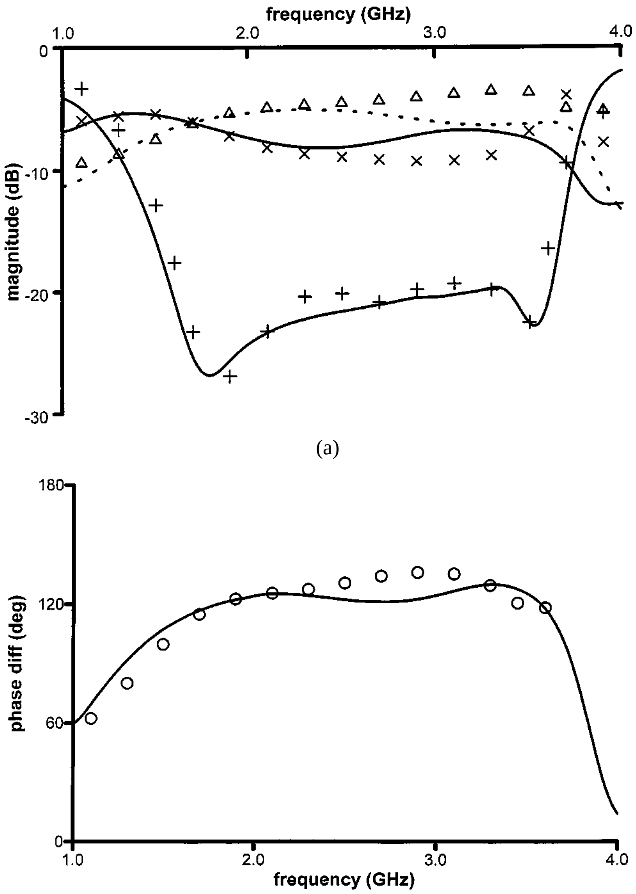

Fig. 2. (a) Magnitudes of scattering coefficients for prototype coupler (with structure and dimensions given in Fig. 1): $|\gamma|$ + + +predicted, — measured, $|\alpha|$ $\Delta\,\Delta\,\Delta$ predicted, — measured, $|\beta|$ $\times\ \times\ \times$ predicted, — measured. (b) Phase difference between coupling coefficients α and β for prototype coupler (with structure and dimensions given in Fig. 1) o o o predicted, — measured.

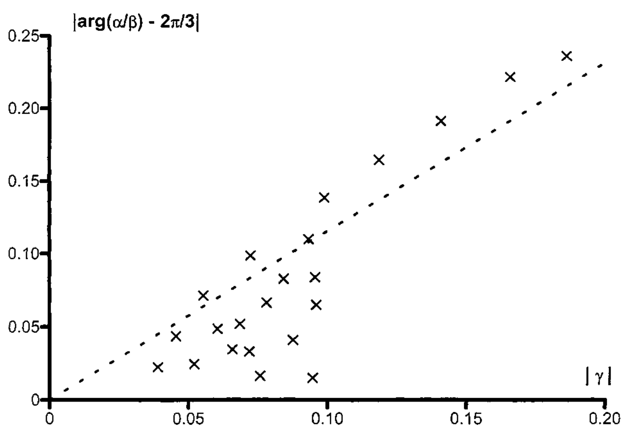

Fig. 3. Using results of Fig. 2 to check range of validity for (11) $\times\ \times\ \times$ measured, - - - line representing $|\arg(\alpha/\beta) - 2\pi/3| = 2|\gamma|/\sqrt{3}$.

from the scatter of the data points for this representative plot that the expressions given in (9)–(11) are valid only when $|\gamma|$ is less than 0.05.

IV. Conclusion

In this paper, we have shown that a simple variation of the double-ring structure proposed by Kim *et al.* [6] allows us to broaden the $|\gamma| < 0.1$ bandwidth of the symmetrical five-port microstrip coupler from the original figure of 58% to the improved value of 76%. The formulas listed in Section II form the basis of the computer-aided-design software we developed for the present project, and the results we obtained confirm that the approximations we utilized to simplify the analysis have not impaired the validity of our model over the frequency range of interest to us.

References

[1] G. P. Riblet and E. R. B. Hansson, "Use of a matched symmetrical five-port junction to make six-port measurements," in *IEEE MTT-S Int. Microwave Symp. Dig.*, 1981, pp. 151–153.

[2] G. Colef, M. Ettenberg, and P. R. Karmel, "Performance of integrated six-port reflectometer operated with pulsed signals," *IEEE Trans. Instrum. Meas.*, vol. 39, pp. 189–194, Feb. 1990.

[3] D. J. Bannister, J. P. Ide, and M. Perkins, "Improved six-port reflectometer based on symmetrical five-port junction," *Electron. Lett.*, vol. 28, pp. 406–408, Feb. 1992.

[4] G. W. Wang, Z. Zhang, K. Lee, and M. Chen, "Simplified configuration of six-port reflectometer based on symmetrical five-port junction," in *Progress Electromag. Res. Symp. Dig.*, 2000, p. 406.

[5] M. D. Abouzahra, "Comments on simple approach to four-way hybrid ring power divider design," *Microwave Opt. Technol. Lett.*, vol. 5, pp. 154–155, Mar. 1992.

[6] D. I. Kim, K. Araki, and Y. Naito, "Properties of symmetrical five-port circuit and its broadband design," *IEEE Trans. Microwave Theory Tech.*, vol. MTT-32, pp. 51–57, Jan. 1984.

[7] F. C. de Ronde, "Octave-wide matched symmetrical reciprocal four- and five-ports," in *IEEE Int. Microwave Symp. Dig.*, 1982, pp. 521–523.

[8] G. P. Riblet, "Internally and externally matched lumped-element symmetrical five-ports," in *European Microwave Conf. Dig.*, 1983, pp. 344–347.

[9] M. Malkomes, H. J. Schmitt, G. Kadisch, and M. van der Poel, "Broadband multiport coupler," in *European Microwave Conf. Dig.*, 1983, pp. 339–343.

[10] K. C. Gupta and M. D. Abouzahra, "Analysis and design of four-port and five-port microstrip disc circuits," *IEEE Trans. Microwave Theory Tech.*, vol. MTT-33, pp. 1422–1428, Dec. 1985.

[11] S. K. Judah and M. D. Judd, "Direct synthesis of matched symmetric five-port junction from its scattering matrix," *Proc. Inst. Elect. Eng.*, pt. H, vol. 133, pp. 95–98, Apr. 1986.

[12] S. P. Yeo, B. Tan, and E. H. Kwek, "Improved design for symmetrical six-port microstrip coupler (based on double-ring-with-star topology)," *IEEE Trans. Microwave Theory Tech.*, vol. 48, pp. 1074–1077, Jun. 2000.

[13] S. P. Yeo and C. L. Lau, "First-order model of symmetrical six-port microstrip coupler," *IEEE Trans. Microwave Theory Tech.*, vol. 39, pp. 1666–1669, Sept. 1991.

[14] R. K. Hoffmann, *Handbook of Microwave Integrated Circuits*. Norwood, MA: Artech House, 1987.

[15] M. Gen and R. Cheng, *Genetic Algorithm and Engineering Design*. New York: Wiley, 1996.

[16] A. J. Belfort and A. L. Cullen, "First-order theory of five-port symmetrical star junction," *Electron. Lett.*, vol. 18, pp. 841–842, Sept. 1982.